JOURNAL OF VIROLOGY, June 2004, p. 5584–5590 Vol. 78, No. 11
0022-538X/04/$08.00+0 DOI: 10.1128/JVI.78.11.5584–5590.2004


# Fatal Disseminated Mouse Adenovirus Type 1 Infection in Mice Lacking B Cells or Bruton's Tyrosine Kinase

Martin L. Moore,[1]† Erin L. McKissic,[2] Corrie C. Brown,[3] John E. Wilkinson,[4] and Katherine R. Spindler[5]*

*Department of Genetics, Franklin College of Arts and Sciences,[1] and Department of Pathology, College of Veterinary Medicine,[3] University of Georgia, Athens, Georgia 30602, and Department of Epidemiology, University of Michigan School of Public Health,[2] and Department of Pathology and Unit for Lab Animal Medicine[4] and Department of Microbiology and Immunology,[5] University of Michigan Medical School, Ann Arbor, Michigan 48109*

Received 8 October 2003/Accepted 26 January 2004

**Mouse adenovirus type 1 (MAV-1) infection of B-cell-deficient and Bruton's tyrosine kinase (Btk)-deficient mice resulted in fatal disseminated disease resembling human adenovirus infections in immunocompromised patients. Mice lacking B cells or Btk were highly susceptible to acute MAV-1 infection, in contrast to controls and mice lacking T cells. To our knowledge, this is the first demonstration that mice with an X-linked immunodeficiency phenotype (Btk deficient) are susceptible to virus-induced disease. Mice lacking B cells or Btk on a C57BL/6 background succumbed with encephalomyelitis, hepatitis, and lymphoid necrosis. Mice lacking B cells on a BALB/c background succumbed with enteritis and hepatitis. Survival of acute MAV-1 infection correlated with early T-cell-independent neutralizing antibody and T-cell-independent antiviral immunoglobulin M. Treatment of MAV-1-infected $Btk^{-/-}$ mice 4 to 9 days postinfection with antiserum harvested 6 to 9 days postinfection from MAV-1-infected $Btk^{+/+}$ mice was therapeutic. Our findings implicate a critical role for B-cell function in preventing disseminated MAV-1 infection, particularly production of early T-cell-independent antiviral immunoglobulin M.**

Human adenoviruses are associated with self-limiting respiratory, conjunctival, and gastrointestinal disease. In immunocompromised people, human adenovirus infection can result in pneumonia, hepatitis, encephalitis, pancreatitis, gastroenteritis, or disseminated disease involving multiple organs (8, 43). Disseminated human adenovirus infection usually results in death. The incidence of disseminated human adenovirus disease is increasing with the increased number of immunocompromised children, and pediatric bone marrow transplant recipients are most at risk (5, 12, 13, 16).

Due to species specificity, human adenovirus pathogenesis is poorly understood. Study of mouse adenovirus type 1 (MAV-1) permits the analysis of a replicating adenovirus in vivo. The outcome of infection depends on the virus dose and mouse strain (15, 26, 33, 40). In outbred and C57BL/6 (B6) mouse strains, MAV-1 infects cells of the monocyte-macrophage lineage and endothelial cells (10, 20, 33). The highest levels of virus are found in the spleen and brain (20, 26, 39). MAV-1-specific cytotoxic T cells peak at 10 days postinfection (d.p.i.) and then decline (18). T cells cause acute immunopathology and are required for survival 9 to 16 weeks postinfection in MAV-1-induced encephalomyelitis (33). Inbred mouse strains susceptible and resistant to MAV-1 are available, and sublethal irradiation of resistant mice renders them susceptible (40). Mice with a severe combined immunodeficiency (SCID) mutation are susceptible to MAV-1 (10, 35).

Here we report findings that survival of acute MAV-1 infection is B-cell dependent and T-cell independent. We postulated that Bruton's tyrosine kinase (Btk) plays a role in protection from MAV-1. Loss of Btk in mice results in the X-linked immunodeficiency (Xid) phenotype (22). $Btk^{-/-}$ mice have reductions in serum immunoglobulin (natural antibody), conventional B cells, and peritoneal B-1 cells relative to control mice (22). Here we demonstrate that Btk is required for survival of MAV-1 infection. We present data indicating that early T-cell-independent antiviral immunoglobulin M (IgM) plays a pivotal role in protection against disseminated MAV-1 infection.

## MATERIALS AND METHODS

**Virus and mice.** Wild-type MAV-1 was propagated and titrated in 3T6 cells (9). The mice used are indicated in Table 1 (11, 14, 23, 24, 29–31). $A^{b}_{\beta}{}^{-/-}$ and Jh mice were purchased from Taconic. C57BL/6NCr (B6) and BALB/CAnNCr mice were purchased from the National Cancer Institute. All other mice were purchased from Jackson Laboratory. The 50% lethal dose ($LD_{50}$) was determined as described previously (37). Sera were heat inactivated at 57°C for 45 min before passive transfer.

**Quantitation of virus.** Organ homogenates were prepared as described previously (40) or in phosphate-buffered saline (PBS) with 1-mm glass beads (BioSpec Products, Bartlesville, Okla.) in 2 ml/well 96-well plates (Axygen, Union City, Calif.) with a Mini Beadbeater (BioSpec) and the manufacturer's protocol. Virus was titrated by plaque assay as described previously (9). The means of the log titers were compared by a two-tailed *t* test. Counts of fewer than 10 plaques/60-mm plate were considered unreliable; thus, $2 \times 10^3$ PFU/g was the detection limit. Values below the detection limit were excluded from statistical analyses.

**Histology and in situ hybridization.** The following organs were formalin fixed: spleen, kidney, liver, small and large intestine, Peyer's patches, thymus, lung, heart, and brain. Tissue sections were stained or processed for in situ hybridiza-

* Corresponding author. Mailing address: University of Michigan Medical School, 1150 W. Medical Center Dr., 6724 Medical Science Bldg. II, Ann Arbor, MI 48109-0620. Phone: (734) 615-2727. Fax: (734) 764-3562. E-mail: krspin@umich.edu.

† Present address: Department of Medicine, Vanderbilt University Medical Center, Nashville, Tenn.

TABLE 1. Mice used in this study

| Strain name | Abbreviation | Defect | Reference |
|---|---|---|---|
| C57BL/6J, C57BL/6NCr | B6 | None | |
| BALB/CAnNCr | BALB/c | None | |
| B6.129S7-Rag1$^{tm1Mom}$ | RAG-1$^{-/-}$ | T- and B-cell deficient | 31 |
| B6.129S2-Igh-6$^{tm1Cgn}$ | μMT | B-cell deficient; B6 background | 25 |
| B6;129S-Btk$^{tm1Wk}$ | Btk$^{-/-}$ | Btk deficient | 24 |
| B6.129S-Tcra$^{tm1Mom}$ | TCRα$^{-/-}$ | α/β T-cell deficient | 30 |
| B6.129P-Tcrb$^{tm1Mom}$Tcrd$^{tm1Mom}$ | TCRβxδ$^{-/-}$ | α/β and γ/δ T-cell deficient | 30 |
| B6.129S6-Cd4$^{tm1Knw}$ | CD4$^{-/-}$ | CD4$^{+}$-T-cell deficient | 29 |
| B6.129-Abb$^{tm1}$N5 | $A^{b}_{\beta}{}^{-/-}$ | MHC class II deficient | 15 |
| C.129(B6)-Jhd$^{tm1}$ | Jh | B-cell deficient; BALB/c background | 12 |

tion as previously described (20) with an antisense digoxigenin-labeled MAV-1 early region 3 riboprobe.

**Neutralizing antibody assay.** Heat-inactivated mouse sera were diluted twofold in $4 \times 10^6$ PFU of MAV-1 per ml and incubated for 1 h at 37°C. Dulbecco's modified Eagle's medium (DMEM) with 5% heat-inactivated calf serum was removed from the wells of a 96-well plate containing confluent 3T6 cells, 25 μl of the virus-serum mixtures (corresponding to a multiplicity of infection of 10) was added to wells in duplicate, and the virus was allowed to adsorb for 1 h at 37°C. DMEM with 1% heat-inactivated calf serum was added, and the wells were monitored for 4 to 6 days for cytopathic effect, given scores of 0 (no cytopathic effect), ½ (some cytopathic effect), or + (complete cytopathic effect). The neutralizing antibody titer was the last dilution exhibiting a less than complete cytopathic effect.

**Enzyme-linked immunosorbent assay.** An MAV-1 stock was precipitated with polyethylene glycol (9). The virus pellet was resuspended in 1× DMEM in 0.01 of the original stock volume. Immulon 2 HB enzyme-linked immunosorbent assay plates (Fisher Scientific) were coated overnight with polyethylene glycol-precipitated MAV-1 diluted 1:100 in PBS or medium diluted 1:20 in PBS. The wells were coated with the same concentration of protein, as determined by a Bradford assay. The plates were washed and blocked with 1% bovine serum albumin, and serial dilutions of serum in PBS were added. Mouse anti-MAV-1 antisera were detected with secondary peroxidase-conjugated goat anti-mouse IgG serum (Amersham) or anti-mouse IgM (BioSource International) with 1-Step Turbo-TMB (Pierce) as the substrate.

**Northern analysis.** Liver samples were homogenized in 900 μl of TRI reagent, and RNA was isolated by the manufacturer's protocol (Molecular Research Center, Inc.). Polyadenylated RNA was isolated with the PolyATract system (Promega); 1 μg of each polyadenylated RNA was electrophoresed on a 1% agarose–3% formaldehyde–40 mM MOPS (morpholinopropanesulfonic acid, pH 7.0)–10 mM sodium acetate–1 mM EDTA gel and then transferred to a nylon membrane (Boehringer Mannheim). For probes, the β-actin 3′ primer (38) and Fas ligand (FasL) probe (45) were end labeled with γ-$^{32}$P by using polynucleotide kinase. Membranes were hybridized, stripped, and reprobed as described previously (21). mRNA levels were quantitated with a Phosphorimager and ImageQuant software (Molecular Dynamics) and compared by a two-tailed *t* test.

## RESULTS

**B-cell- and Btk-deficient mice are highly susceptible to MAV-1 infection.** MAV-1 induces dose-dependent encephalomyelitis in B6 mice (15). We first assessed the role of T and B cells in MAV-1 disease by using immunodeficient mice on a B6 background. RAG-1$^{-/-}$ mice, which lack T and B cells, were more susceptible to MAV-1 infection than B6 controls (Fig. 1A). These data are consistent with published results for CB.17/SCID (35) and BALB/SCID (10) mice, which also lack T and B cells. To determine the relative contributions of T and B cells to protection against MAV-1, we infected mice lacking T cells (TCRβxδ$^{-/-}$) and mice lacking B cells (μMT). μMT mice were highly susceptible to MAV-1 infection, whereas TCRβxδ$^{-/-}$ mice survived, like the controls (Fig. 1B). T-cell-deficient mice exhibit fewer acute MAV-1 disease signs than controls, and T-cell-mediated acute immunopathology in MAV-1 disease is perforin and major histocompatibility complex class I dependent (33). Thus, B cells but not T cells were required for survival of B6 mice after acute MAV-1 infection.

MAV-1 does not cause encephalomyelitis in BALB/c mice, which are more resistant to MAV-1 infection than B6 mice (15). To test whether the B-cell requirement for survival in μMT mice is specific to the B6 background, we infected B-cell-deficient mice (Jh) on a BALB/c background. Jh mice were highly susceptible to MAV-1 infection (Fig. 1C).

Since survival of acute MAV-1 infection was B-cell dependent and T-cell independent (Fig. 1B), we hypothesized that Btk plays a role in protection from MAV-1-induced disease. Btk$^{-/-}$ mice were highly susceptible to MAV-1 infection (Fig. 1C and D). The $LD_{50}$ of Btk$^{-/-}$ mice was 0.1 PFU. This corresponds to 100 virus particles, because the MAV-1 particle/PFU ratio is ≈1,000 in 3T6 cells (data not shown). Although Btk$^{-/-}$ mice are on a mixed B6 and 129 genetic background, the $LD_{50}$s for B6 and 129 mice are the same ($>10^{4.4}$ PFU) (40). Thus, Btk is required for survival of MAV-1 infection. To our knowledge, this is the first demonstration that Btk plays a role in protection from virus-induced disease in mice.

**B-cell and Btk deficiencies result in systemically high viral loads.** We determined virus loads in the organs of MAV-1-infected B-cell-deficient, Btk-deficient, and control mice by

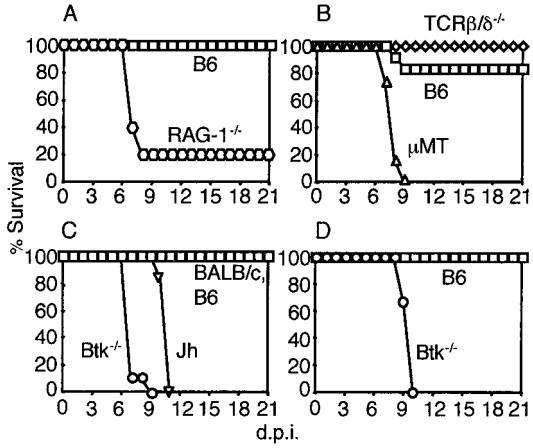


FIG. 1. Survival of (A) B6 ($n = 3$) and RAG-1$^{-/-}$ ($n = 5$), (B) B6 ($n = 6$), μMT ($n = 6$), and TCRβxδ$^{-/-}$ ($n = 6$), (C) B6 ($n = 6$), BALB/c ($n = 6$), Btk$^{-/-}$ ($n = 9$), and Jh ($n = 6$), and (D) B6 ($n = 3$) and Btk$^{-/-}$ ($n = 6$) mice. Mice were injected intraperitoneally with (A) 100 PFU, (B) 700 PFU, (C) 700 PFU, and (D) 1 PFU.

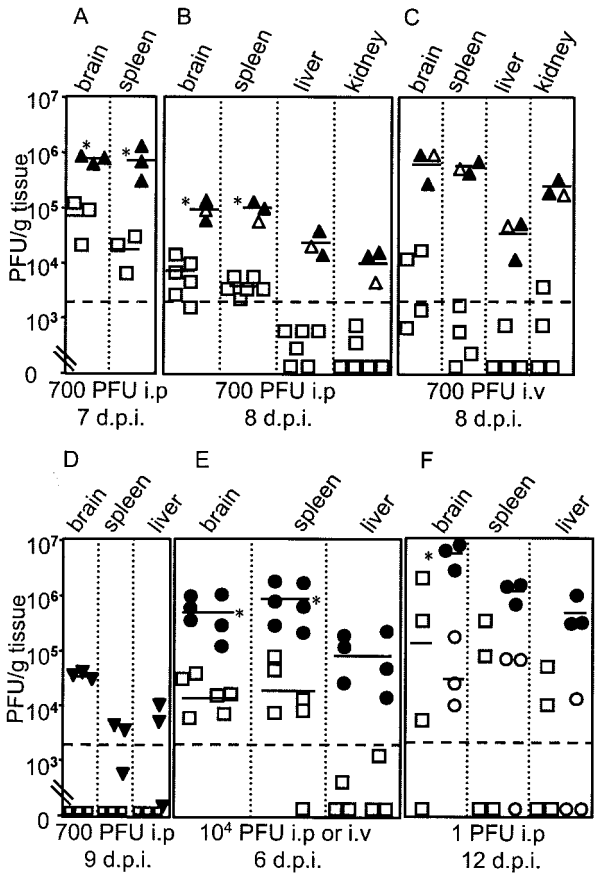


FIG. 2. Quantitation of virus from (A to C) B6 and μMT, (D) BALB/c and Jh, and (E and F) B6 and Btk$^{-/-}$ mice; (E) three mice each were infected intraperitoneally or intravenously (symbols to the left and right, respectively, in each group). Each symbol represents an individual mouse. B6, □; μMT, △; BALB/c, □; Jh, ▽; Btk$^{-/-}$, ○. Solid symbols, mice that were moribund when euthanized. The short horizontal lines indicate means for three or more log-transformed titers; the dotted line at $2 \times 10^3$ PFU/g indicates the limit of detection. *, $P < 0.01$; in panel F the asterisk relates to moribund Btk$^{-/-}$ mice compared to B6 mice and to Btk$^{-/-}$ mice not showing disease signs.

plaque assay. MAV-1 titers were higher in the brain, spleen, liver, and kidney of μMT mice than in controls, and μMT mice had a more disseminated infection (Fig. 2A to C). MAV-1-infected BALB/c mice had no detectable virus at 9 d.p.i, whereas Jh mice had virus in the brain, spleen, and liver (Fig. 2D). The viral loads in the organs of mice infected intraperitoneally or intravenously with $10^4$ PFU were significantly higher in Btk$^{-/-}$ mice than B6 mice (Fig. 2E). Infection of B-cell- and Btk-deficient mice intravenously or intranasally with MAV-1 resulted in lethality and high viral loads (Fig. 2C and E, and data not shown). At 12 d.p.i. with 1 PFU, viral loads were higher in moribund Btk$^{-/-}$ mice than in B6 or Btk$^{-/-}$ mice not showing disease signs (Fig. 2F). Taken together, the results were that mice deficient for B cells or Btk had elevated MAV-1 titers and disseminated infection, and this correlated with death.

**MAV-1 induces hepatitis, encephalomyelitis, and lymphoid necrosis in μMT and Btk$^{-/-}$ mice and induces hepatitis and enteritis in Jh mice.** We examined the histological consequences of fatal MAV-1 disease in mice lacking B cells or Btk at 7 d.p.i. There was perivascular edema in the brains of infected control B6 mice (inset, Fig. 3A), but the spleen, liver, and small intestine appeared unaffected (Fig. 3B to D). In comparison, μMT and Btk$^{-/-}$ mice had perivascular edema and also vascular degeneration in the brain, evident by perivascular fibrin deposition (Fig. 3E and I), and there was significant hepatic necrosis (Fig. 3G and K). In moribund B6 mice given high doses of MAV-1, vascular degeneration in the brain has been observed, but not liver pathology (15; M. L. Moore and K. R. Spindler, unpublished data). The spleens of μMT and Btk$^{-/-}$ mice showed lymphoid necrosis (Fig. 3F and J) that was not seen in B6 controls at this does (700 PFU). However, at higher doses of MAV-1, splenic necrosis has been observed in B6 mice (15; M. L. Moore and K. R. Spindler, unpublished data). In situ hybridization-positive staining of endothelial cells is shown for each organ in which it was observed (insets, Fig. 3A to L). Overall, the B-cell- and Btk-deficient mice had more disseminated disease than B6 controls.

Analysis of tissues taken at 9 d.p.i. from control BALB/c and moribund Jh mice infected with 700 PFU (same mice as shown in Fig. 2D) revealed that Jh mice succumbed with hemorrhagic enteritis and hepatic necrosis (Fig. 3M to T). Enteritis has been observed in MAV-1-infected outbred and BALB/SCID mice (10, 26). Typical MAV-1 inclusion bodies were seen in hematoxylin- and eosin-stained small intestine (Fig. 3T). Interestingly, like μMT mice, Jh mice had elevated viral titers in brain (Fig. 2D), but unlike μMT mice, Jh mice had no brain pathology (Fig. 3Q), suggesting that host factors contributing to MAV-1 pathogenesis in B-cell-deficient mice are strain specific. The Peyer's patches and spleen lymphoid follicles of infected control BALB/c mice were activated; they had defined germinal centers (Fig. 3N and P). In contrast, the spleens of infected Jh mice appeared disorganized but had no necrosis (Fig. 3R). B-cell-deficient mice on the BALB/c background thus showed more disease than BALB/c controls.

Analysis of tissues taken at 12 d.p.i. from B6 and Btk$^{-/-}$ mice that had been mock infected or infected with the low dose of 1 PFU (same mice as shown in Fig. 2F) revealed cellular inflammation in the infected mice of both mouse strains, though it was more extensive in Btk$^{-/-}$ mice (Fig. 4). Infected B6 mice had vasculitis in the brain (Fig. 4D) and defined germinal centers in the spleen (Fig. 4E). Moribund Btk$^{-/-}$ mice had vasculitis, meningeal vascular necrosis, and vascular degeneration in the brain (Fig. 4J and data not shown); their spleens had excessive lymphoid necrosis (Fig. 4K), and their livers had significant lymphoplasmacytic hepatitis (Fig. 4L).

**FasL mRNA levels were altered in MAV-1-infected Jh mice.** BALB/SCID and CB.17/SCID mice are susceptible to MAV-1 infection, and MAV-1 targets the liver in these mice (10, 35). However, hepatic disease induced by MAV-1 in CB.17/SCID mice resembled Reye's syndrome; there was no significant hepatic necrosis or inflammation (35). In contrast, MAV-1-infected Jh mice exhibited significant hepatic necrosis (Fig. 3S) resembling acute human adenovirus hepatitis in immunosuppressed patients (44). Since T cells are present in Jh mice but not BALB/SCID mice, we hypothesized that T cells contribute to acute hepatitis in MAV-1-infected Jh mice. To address this hypothesis, we analyzed the mRNA levels of genes associated with T-cell function in the liver. The Fas/FasL pathway is an

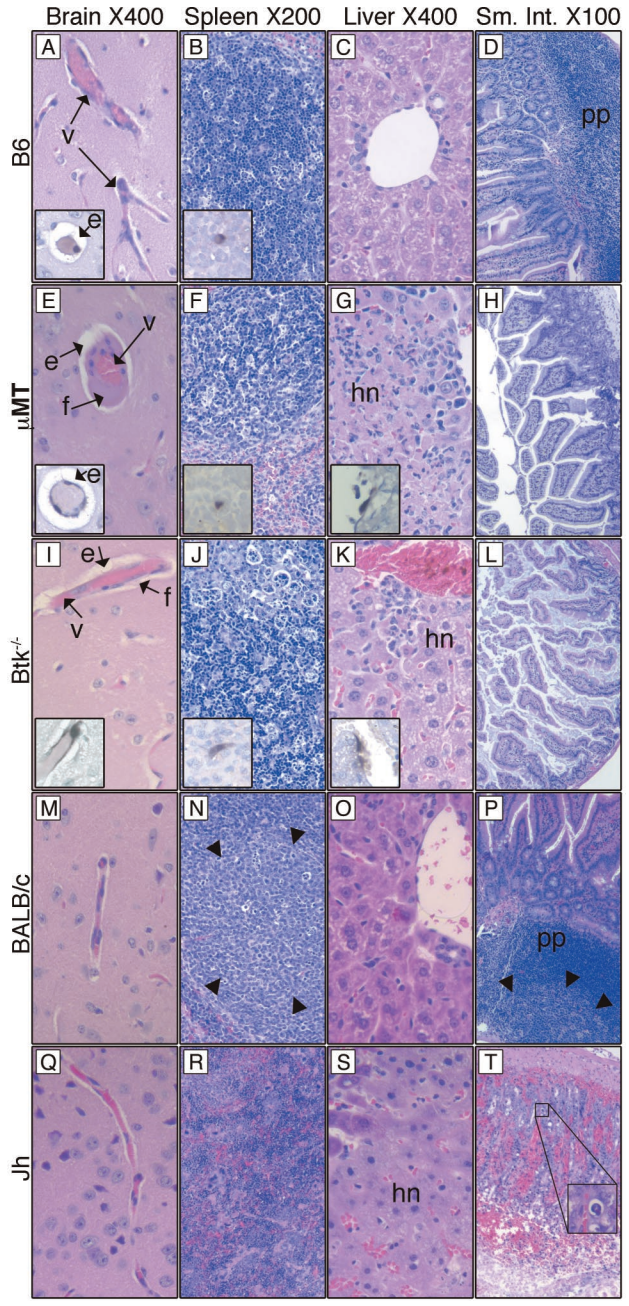


FIG. 3. (A to L) Organs taken at 7 d.p.i. from B6, μMT, and Btk$^{-/-}$ mice infected with 700 PFU. Tissue sections were stained with hematoxylin and eosin or processed for in situ hybridization. Insets (magnification, 400×) show endothelial cells of the same organ stained positively with a viral in situ hybridization probe. (M to T) Organs taken at 9 d.p.i. from BALB/c and Jh mice infected with 700 PFU. Tissue sections were stained with hematoxylin and eosin. Arrowheads in N and P show the boundary of germinal centers. The inset in panel T is a 400× view of the boxed area showing a viral inclusion body. e, perivascular edema; f, fibrin in the perivascular space; hn, hepatic necrosis; pp, Peyer's patch; v, blood vessel.

important mechanism of T-cell-mediated cytotoxicity (19). We found that FasL liver mRNA levels were induced in infected Jh mice but not control BALB/c mice (Fig. 5). These results are consistent with T cells' contributing to hepatitis in Jh mice.

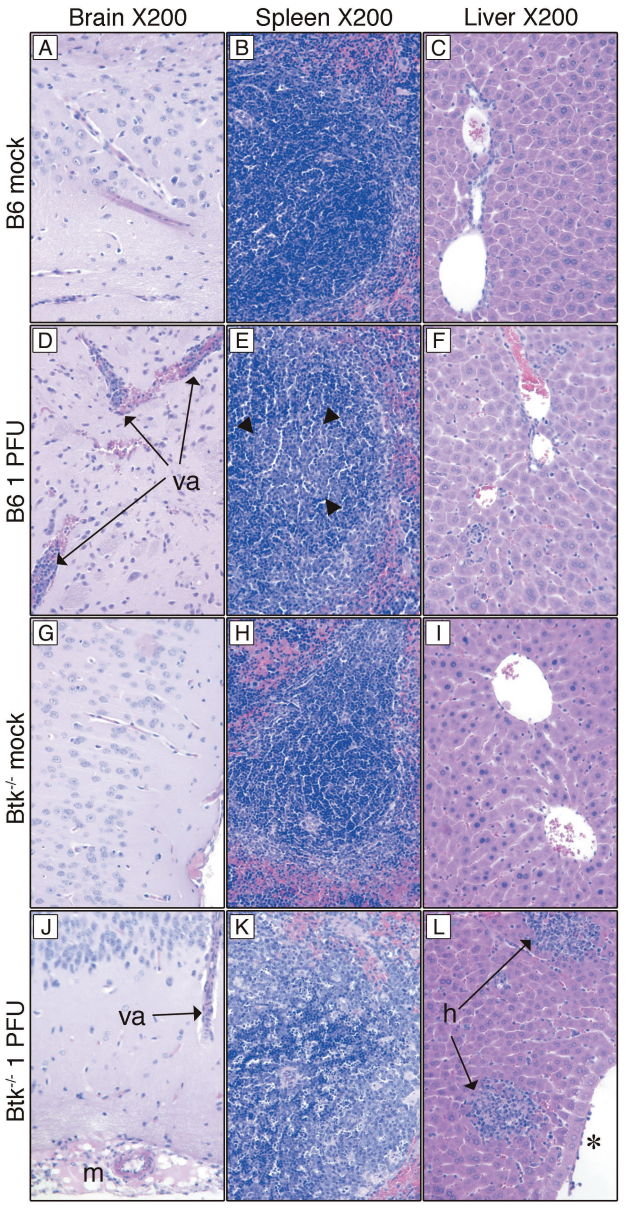


FIG. 4. Representative hematoxylin- and eosin-stained tissue sections from organs taken at 12 d.p.i. from B6 and Btk$^{-/-}$ mice that had been mock infected or infected with 1 PFU. Arrowheads in E show the germinal center boundary. *, lymphocytes adherent to endothelial cells. va, vasculitis; m, meningeal vascular necrosis; h, hepatitis.

**Early T-cell-independent antibody correlates with survival of acute MAV-1 infection.** We analyzed the humoral immune response to MAV-1. There was an increase in neutralizing antibody titer and antiviral IgM 6 d.p.i. in the sera of B6 and T-cell-deficient mice but not Btk$^{-/-}$ mice after infection with $10^4$ PFU (Fig. 6A and 7A, same mice as shown in Fig. 2E). Similarly, T-cell-independent antiviral IgM was detected 6 d.p.i. in B6 and T-cell-deficient mice infected with a lower dose, 700 PFU (Fig. 7B). Antiviral IgG levels were low or undetectable in the sera shown in Fig. 7A and B (data not shown). Sera of B6 but not Btk$^{-/-}$ mice infected with 700 PFU (same mice as Fig. 1C) had neutralizing antibody titers at

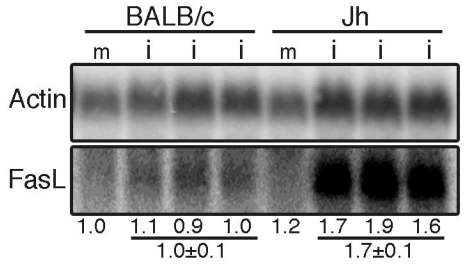


FIG. 5. Northern analysis of FasL polyadenylated RNA in BALB/c and Jh liver. RNA isolated 9 d.p.i. from the liver of BALB/c and Jh mice that had been mock infected (m) or infected (i) with 700 PFU. Each lane has RNA from an individual mouse. The level of FasL was normalized to the actin level and then to the value for the mock-infected BALB/c mouse, as indicated under the lanes. FasL levels were higher in infected Jh than BALB/c livers ($P = 0.002$).

7 d.p.i. (Fig. 6B). Neutralizing antibody was induced in major histocompatibility complex class II-deficient ($A_\beta^{b-/-}$) and control mice (Fig. 6C). B6 mice infected with 1 PFU produced neutralizing antibody antiviral IgM and IgG at 12 d.p.i, whereas $Btk^{-/-}$ mice did not (Fig. 6D and 7C, same mice as in Fig. 2F). At 12 weeks postinfection, major histocompatibility complex class II was required for anti-MAV-1 IgG, whereas CD4 was dispensable (Fig. 7D). Interestingly, $A_\beta^{b-/-}$ and $CD4^{-/-}$ mice survive to 12 weeks postinfection, like controls (33); thus, antiviral IgG is not required for survival of MAV-1 infection. Taken together, the results show that T-cell-independent antiviral IgM and T-cell-independent neutralizing antibody correlated with survival of acute MAV-1 infection, whereas the absence of antiviral IgG had no effect on survival.

**Passive transfer of immune antisera protects RAG-$1^{-/-}$ and $Btk^{-/-}$ mice from MAV-1 infection.** We first tested whether neutralizing antibody or natural antibody could protect RAG-$1^{-/-}$ mice from MAV-1 infection. Treatment of $RAG^{-/-}$ mice with naïve B6 serum (natural antibody) on days 0 to 7 postinfection had no effect on virus loads, whereas treatment with MAV-1-immune serum reduced them significantly (Fig. 8A). We then tested whether early neutralizing antibody could protect MAV-1-infected $Btk^{-/-}$ mice. Treatment at 4 to 9 d.p.i. with serum from 6- to 9-day-infected mice that had both antiviral IgM and IgG (Fig. 8B) protected three of four $Btk^{-/-}$ mice (Fig. 8C).

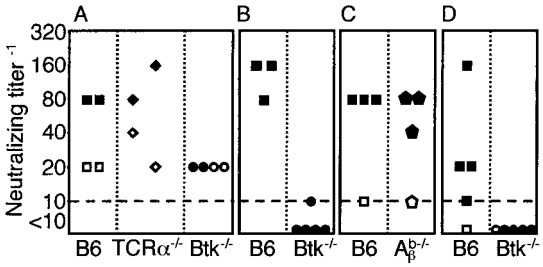


FIG. 6. Serum neutralizing antibody titers. Sera obtained (A) pre-infection (open symbols) and at 6 d.p.i. (solid symbols) from B6, $TCR\alpha^{-/-}$, and $Btk^{-/-}$ mice that had been infected with $10^4$ PFU, (B) 7 d.p.i. from B6 and $Btk^{-/-}$ mice that had been infected with 700 PFU, (C) 9 d.p.i. from B6 and $A_\beta^{b-/-}$ mice that had been mock infected (open symbols) or infected (solid symbols) with 700 PFU, and (D) 12 d.p.i. from B6 and $Btk^{-/-}$ mice that had been mock infected (open symbols) or infected (solid symbols) with 1 PFU of MAV-1. The dotted line represents the limit of detection. Each symbol represents serum from an individual mouse.

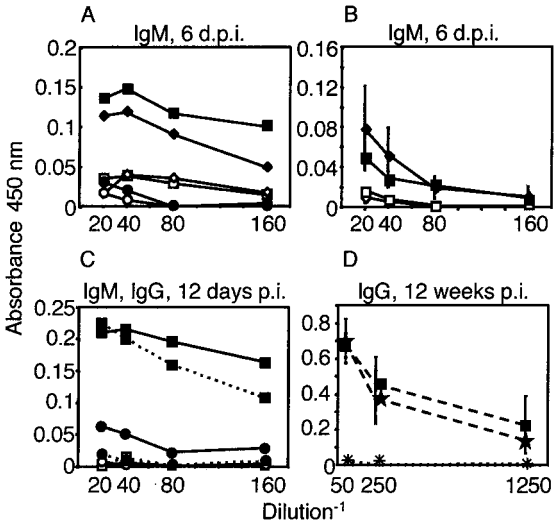


FIG. 7. Anti-MAV-1 IgM and IgG. (A) Pooled sera preinfection (open symbols) and 6 d.p.i. (solid symbols) from B6 (□, $n = 3$), $TCR\alpha^{-/-}$ (◇, $n = 5$), and $Btk^{-/-}$ (○, $n = 2$) mice infected with $1 \times 10^4$ PFU assayed for antiviral IgM. (B) Sera obtained preinfection (open symbols) and 6 d.p.i. (solid symbols) from five B6 and five $TCR\beta x\delta^{-/-}$ mice infected with 700 PFU assayed for antiviral IgM. Mean values ± standard deviation are shown. (C) Sera from mock-infected B6 (□, $n = 1$) or $Btk^{-/-}$ (○, $n = 1$) mice and pooled sera from B6 (■, $n = 4$) and $Btk^{-/-}$ (●, $n = 6$) mice infected with 1 PFU were assayed for antiviral IgM (solid lines) and antiviral IgG (dashed lines) at 12 d.p.i. (D) Mean values for sera from five B6 (■) mice and five $CD4^{-/-}$ (★) mice, pooled sera from 5 $A_\beta^{b-/-}$ (+) mice, and pooled sera from two $TCR\beta x\delta^{-/-}$ (×) mice assayed for antiviral IgG at 12 weeks p.i. with 700 PFU. Mean values ± standard deviation are shown for B6 and $CD4^{-/-}$ samples.

## DISCUSSION

We demonstrated here a crucial role for B cells and Btk in preventing fatal disseminated MAV-1 disease. This parallels the observations, albeit from a small number of patients, that Btk-deficient people suffer adverse effects after human adenovirus infection (25, 27, 28). B-cell- and Btk-deficient mice were highly susceptible to MAV-1 and succumbed with high viral loads and disseminated infection (Fig. 1 and 2). This suggests that Btk may be an integral component of the immune response to adenoviruses.

Infection of B-cell- or Btk-deficient mice with MAV-1 resulted in hepatitis (Fig. 3G, K, and S) that was histologically similar to human adenovirus hepatitis in immunocompromised patients (6, 7, 44). μMT and $Btk^{-/-}$ mice infected with 700 PFU succumbed with hepatic necrosis and mild cellular inflammation (Fig. 3G and K). MAV-1 endothelial cell tropism (insets, Fig. 3G and K) was consistent with previous findings for mice with a B6 or 129 background (10, 15) (data not shown). $Btk^{-/-}$ mice infected with as little as 1 PFU also succumbed with hepatic necrosis but had significant cellular inflammation (Fig. 4L). Thus, the pathology of MAV-1 hepatitis in $Btk^{-/-}$ mice depended on the virus dose and presum-

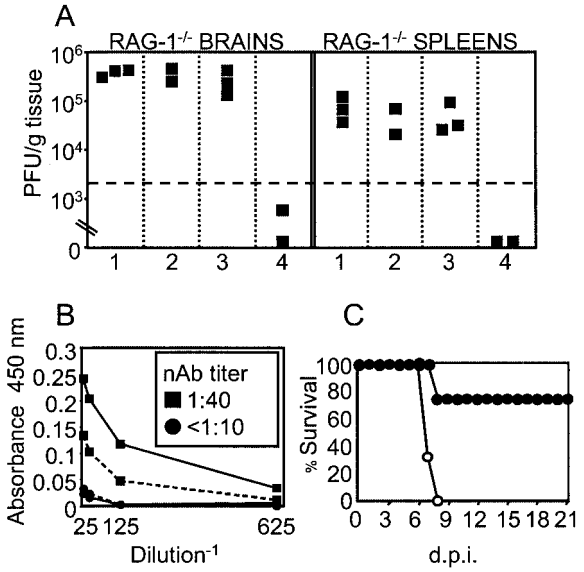


FIG. 8. (A) RAG-1$^{-/-}$ mice infected with 100 PFU were treated intravenously daily on days 0 to 7 postinfection with 0.25 ml of PBS, pooled sera from naïve RAG-1$^{-/-}$ mice, pooled sera from naïve B6 mice, or pooled MAV-1-immune sera diluted 1:4 in PBS (panels 1 to 4, respectively). MAV-1-immune sera were harvested 12 weeks postinfection from B6 mice infected with 700 PFU and had neutralizing antibody titers of >1:1,000, high levels of antiviral IgG, and no detectable antiviral IgM (data not shown and Fig. 5B). Virus levels were determined at 7 d.p.i. (B) Sera pooled from days 6 to 9 postinfection from MAV-1-infected Btk$^{+/+}$ (■) or Btk$^{-/-}$ (●) mice were assayed for antiviral IgM (solid line), IgG (dashed line), and neutralizing antibody (box). (C) Btk$^{-/-}$ mice infected with 100 PFU were treated intraperitoneally daily from days 4 to 9 postinfection with 0.1 ml of the Btk$^{+/+}$ (●, $n = 4$) or Btk$^{-/-}$ (○, $n = 3$) antiserum shown in panel B.

ably the kinetics of inflammation. In contrast, Jh mice (B-cell deficient on a BALB/c background) infected with 700 PFU succumbed with confluent, glassy hepatic necrosis without inflammation (Fig. 3S). MAV-1 inclusion bodies were seen in hepatocytes of Jh but not μMT mice (data not shown) and have been observed in the hepatocytes of infected BALB/SCID and CB.17/SCID mice (10, 35). It is likely that the host genetic background contributed to the differences in cell and organ tropism and pathology observed in MAV-1-infected μMT and Jh mice. Residual B cells in μMT mice (34) may also have contributed to the phenotypic differences.

We hypothesize that T cells play a key role in MAV-1 hepatitis because the virus induces hepatitis in B-cell-deficient but not SCID (T-cell and B-cell deficient) mice (10, 35) (Fig. 2G and S). Furthermore, mice lacking T cells succumb to MAV-1 infection 9 to 16 weeks postinfection with encephalomyelitis and MAV-1 dissemination to the liver but no liver pathology (33). T-cell function may be defective in MAV-1-infected B-cell-deficient mice, as is the case for lymphocytic choriomeningitis virus-infected μMT mice (17). FasL mRNA levels were higher in MAV-1-infected Jh livers than BALB/c livers (Fig. 5). Further experiments are needed to assess the role of the Fas/FasL cytolytic pathway in MAV-1-induced hepatitis. FasL contributes to lymphocytic choriomeningitis virus-induced hepatitis (1). Our data are consistent with a model in which early T-cell-independent antiviral IgM plays a pivotal role in protection against MAV-1 infection. In the absence of such IgM (in B-cell or Btk deficient mice), a disseminated infection ensues in which T cells induce immunopathology. Experiments testing the role of T cells and FasL in MAV-1 hepatitis may reveal an immunoregulatory role for early T-cell-independent antibody.

Early T-cell-independent neutralizing antibody and T-cell-independent antiviral IgM correlated with survival of acute MAV-1 infection (Fig. 6 and 7). In contrast, the absence of anti-MAV-1 IgG had no effect on survival (33) (Fig. 7D). Antigens that activate B cells in the absence of T cells have been classified into two groups based on whether they induce antibody in Xid mice (TI-1) or not (TI-2) (32). Polyomavirus is a TI-2 antigen and elicits protective T-cell-independent IgM and IgG in T-cell-deficient mice (41, 42). Our results showed that MAV-1 behaves like a TI-2 antigen (Fig. 6 and 7). Natural and early virus-induced IgM contributes to protection against influenza virus (3). However, in contrast to MAV-1 infection, μMT and Btk-deficient mice are not susceptible to polyomavirus- or influenza virus-induced disease (4, 36). Baumgarth has proposed that T-cell-independent IgM regulates B-cell activation (2). MAV-1 may be useful for testing this model.

MAV-1 infection of B-cell- and Btk-deficient mice resulted in high viral loads, disseminated infection, hepatitis resembling human adenovirus-induced hepatitis in immunocompromised humans, and lethality. Our data indicate that early T-cell-independent neutralizing antibody and T-cell-independent IgM play a crucial role in protection from disseminated MAV-1 infection. Treatment of MAV-1-infected Btk$^{-/-}$ mice with early antiviral antiserum had a significant effect on mortality (Fig. 8B and C). Though modestly neutralizing in vitro (Fig. 8B), early antibody (e.g., IgM) may have potent antiviral and/or immunostimulatory potential in vivo.

## ACKNOWLEDGMENTS

We thank James Stanton, Adriana Kajon, Carla Sturkie, Lei Fang, Katie Kempke, and Amanda Welton for technical assistance. We thank Mike Imperiale, Gary Huffnagle, and Rosemary Rochford for critical reviews of the manuscript.

This work was supported by NIH grant R01 AI023762 to K.R.S. and by an NIH predoctoral traineeship (GM 07103) and an ARCS Foundation Scholarship to M.L.M.

## REFERENCES

1. **Balkow, S., A. Kersten, T. T. Tran, T. Stehle, P. Grosse, C. Museteanu, O. Utermohlen, H. Pircher, F. von Weizsacker, R. Wallich, A. Mullbacher, and M. M. Simon.** 2001. Concerted action of the FasL/Fas and perforin/granzyme A and B pathways is mandatory for the development of early viral hepatitis but not for recovery from viral infection. J. Virol. **75:**8781–8791.
2. **Baumgarth, N.** 2000. A two-phase model of B-cell activation. Immunol. Rev. **176:**171–180.
3. **Baumgarth, N., O. C. Herman, G. C. Jager, L. E. Brown, L. A. Herzenberg, and J. Chen.** 2000. B-1 and B-2 cell-derived immunoglobulin M antibodies are nonredundant components of the protective response to influenza virus infection. J. Exp. Med. **192:**271–280.
4. **Berke, Z., H. Mellin, S. Heidari, T. Wen, A. Berglof, G. Klein, and T. Dalianis.** 1998. Adult X-linked immunodeficiency (XID) mice, IGM-/- single knockout and IGM-/-CD8-/- double knockout mice do not clear polyomavirus infection. In Vivo **12:**143–148.
5. **Blanke, C., C. Clark, E. R. Broun, G. Tricot, I. Cunningham, K. Cornetta, A. Hedderman, and R. Hromas.** 1995. Evolving pathogens in allogeneic bone marrow transplantation: increased fatal adenoviral infections. Am. J. Med. **99:**326–328.
6. **Cames, B., J. Rahier, G. Burtomboy, J. de Ville de Goyet, R. Reding, M. Lamy, J. B. Otte, and E. M. Sokal.** 1992. Acute adenovirus hepatitis in liver transplant recipients. J. Pediatr. **120:**33–37.
7. **Carmichael, G. P., J. M. Zahvadnik, and G. H. Moyer.** 1979. Adenovirus

hepatitis in an immunosuppressed adult patient. Am. J. Clin. Pathol. **71:**352–355.
8. **Carrigan, D. R.** 1997. Adenovirus infections in immunocompromised patients. Am. J. Med. **102:**71–74.
9. **Cauthen, A. N., and K. R. Spindler.** 1999. Construction of mouse adenovirus type 1 mutants, p. 85–103. *In* W. S. M. Wold (ed.), Adenovirus methods and protocols. Humana Press, Totowa, N.J.
10. **Charles, P. C., J. D. Guida, C. F. Brosnan, and M. S. Horwitz.** 1998. Mouse adenovirus type-1 replication is restricted to vascular endothelium in the CNS of susceptible strains of mice. Virology **245:**216–228.
11. **Chen, J., M. Trounstine, F. W. Alt, F. Young, C. Kurahara, J. F. Loring, and D. Huszar.** 1993. Immunoglobulin gene rearrangement in B cell deficient mice generated by targeted deletion of the JH locus. Int. Immunol. **5:**647–656.
12. **Flomenberg, P., J. Babbitt, W. R. Drobyski, R. C. Ash, D. R. Carigan, G. V. Sedmak, T. McAuliffe, B. Camitta, M. M. Horowitz, N. Bunin, and J. T. Casper.** 1994. Increasing incidence of adenovirus disease in bone marrow transplant recipients. J. Infect. Dis. **169:**775–781.
13. **Gavin, P. J., and B. Z. Katz.** 2002. Intravenous ribavirin treatment for severe adenovirus disease in immunocompromised children. Pediatrics **110:**1–8.
14. **Grusby, M. J., H. J. Auchincloss, R. Lee, R. S. Johnson, J. P. Spencer, M. Zulstra, R. Jaenisch, V. E. Papaionnou, and L. H. Glimcher.** 1993. Mice lacking major histocompatibility complex class I and class II molecules. Proc. Natl. Acad. Sci. USA **90:**3913–3917.
15. **Guida, J. D., G. Fejer, L.-A. Pirofski, C. F. Brosnan, and M. S. Horwitz.** 1995. Mouse adenovirus type 1 causes a fatal hemorrhagic encephalomyelitis in adult C57BL/6 but not BALB/c mice. J. Virol. **69:**7674–7681.
16. **Hale, G. A., H. E. Heslop, R. A. Krance, M. A. Brenner, D. Jayawardene, D. K. Srivastava, and C. C. Patrick.** 1999. Adenovirus infection after pediatric bone marrow transplantation. Bone Marrow Transplant. **23:**277–282.
17. **Homann, D., A. Tishon, D. P. Berger, W. O. Weigle, M. G. von Herrath, and M. B. Oldstone.** 1998. Evidence for an underlying CD4 helper and CD8 T-cell defect in B-cell-deficient mice: failure to clear persistent virus infection after adoptive immunotherapy with virus-specific memory cells from muMT/muMT mice. J. Virol. **72:**9208–9216.
18. **Inada, T., and H. Uetake.** 1980. Cell-mediated immunity to mouse adenovirus infection: blocking of macrophage migration inhibition and T cell-mediated cytolysis of infected cells by anti-S antigen or anti-alloantigen serum. Microbiol. Immunol. **24:**525–535.
19. **Kagi, D., F. Vignaux, B. Ledermann, K. Burki, V. Depraetere, S. Nagata, H. Hengartner, and P. Golstein.** 1994. Fas and perforin pathways as major mechanisms of T cell-mediated cytotoxicity. Science **265:**528–530.
20. **Kajon, A. E., C. C. Brown, and K. R. Spindler.** 1998. Distribution of mouse adenovirus type 1 in intraperitoneally and intranasally infected adult outbred mice. J. Virol. **72:**1219–1223.
21. **Kajon, A. E., and K. R. Spindler.** 2000. Mouse adenovirus type 1 replication *in vitro* is resistant to interferon. Virology **274:**213–219.
22. **Khan, W. N., F. W. Alt, R. M. Gerstein, B. A. Malynn, I. Larsson, G. Rathbun, L. Davidson, S. Muller, A. B. Kantor, L. A. Herzenberg, F. S. Rosen, and P. Sideras.** 1995. Defective B cell development and function in Btk-deficient mice. Immunity **3:**283–299.
23. **Khan, W. N., P. Sideras, F. S. Rosen, and F. W. Alt.** 1995. The role of Bruton's tyrosine kinase in B-cell development and function in mice and man. Ann. N. Y. Acad. Sci. **764:**27–38.
24. **Kitamura, D., J. Roes, R. Kühn, and K. Rajewsky.** 1991. A B cell-deficient mouse by targeted disruption of the membrane exon of the immunoglobulin μ chain gene. Nature **350:**423–426.
25. **Kozlowski, C., and D. I. K. Evans.** 1991. Neturopenia associated with X-linked agammaglobulinaemia. J. Clin. Pathol. **44:**388–390.
26. **Kring, S. C., C. S. King, and K. R. Spindler.** 1995. Susceptibility and signs associated with mouse adenovirus type 1 infection of adult outbred Swiss mice. J. Virol. **69:**8084–8088.
27. **Lederman, H. M., and J. A. Winkelstein.** 1985. X-Linked agammaglobulinemia: an analysis of 96 patients. Medicine **64:**145–156.
28. **Liese, J. G., W. Wintergerst, K. D. Tympner, and B. H. Belohradsky.** 1992. High- vs. low-dose immunoglobulin therapy in the long-term treatment of X-linked agammaglobulinemia. Am. J. Dis. Child. **146:**335–339.
29. **McCarrick, J. W., III, J. R. Parnes, R. H. Seong, D. Solter, and B. B. Knowles.** 1993. Positive-negative selection gene targeting with the diphtheria toxin A-chain gene in mouse embryonic stem cells. Transgenic Res. **2:**183–190.
30. **Mombaerts, P., A. R. Clarke, M. A. Rudnicki, J. Iacomini, S. Itohara, J. J. Lafaille, L. Wang, Y. Ichikawa, R. Jaenisch, M. L. Hooper, and S. Tonegawa.** 1992. Mutations in T-cell antigen receptor genes α and β block thymocyte development at different stages. Nature **360:**225–231.
31. **Mombaerts, P., J. Iacomini, R. S. Johnson, K. Herrup, S. Tonegawa, and V. E. Papaionnou.** 1992. RAG-1-deficient mice have no mature B and T lymphocytes. Cell **68:**869–877.
32. **Mond, J. J., I. Scher, D. E. Mosier, M. Baese, and W. E. Paul.** 1978. T-independent responses in B cell-defective CBA/N mice to Brucella abortus and to trinitrophenyl (TNP) conjugates of Brucella abortus. Eur. J. Immunol. **8:**459–463.
33. **Moore, M. L., C. C. Brown, and K. R. Spindler.** 2003. T cells cause acute immunopathology and are required for long-term survival in mouse adenovirus type 1-induced encephalomyelitis. J. Virol. **77:**10060–10070.
34. **Orinska, Z., A. Osiak, J. Lohler, E. Bulanova, V. Budagian, I. Horak, and S. Bulfone-Paus.** 2002. Novel B cell population producing functional IgG in the absence of membrane IgM expression. Eur. J. Immunol. **32:**3472–3480.
35. **Pirofski, L., M. S. Horwitz, M. D. Scharff, and S. M. Factor.** 1991. Murine adenovirus infection of SCID mice induces hepatic lesions that resemble human Reye syndrome. Proc. Natl. Acad. Sci. USA **88:**4358–4362.
36. **Reale, M. A., C. A. Bona, and J. L. Schulman.** 1985. Isotype profiles of anti-influenza virus antibodies in mice bearing the *xid* defect. J. Virol. **53:**425–429.
37. **Reed, L. J., and H. Muench.** 1938. A simple method of estimating fifty per cent endpoints. Am. J. Hyg. **27:**493–497.
38. **Schmitt, R. M., E. Bruyns, and H. R. Snodgrass.** 1991. Hematopoietic development of embryonic stem cells in vitro: cytokine and receptor gene expression. Genes Dev. **5:**728–740.
39. **Smith, K., C. C. Brown, and K. R. Spindler.** 1998. The role of mouse adenovirus type 1 early region 1A in acute and persistent infections in mice. J. Virol. **72:**5699–5706.
40. **Spindler, K. R., L. Fang, M. L. Moore, C. C. Brown, G. N. Hirsch, and A. K. Kajon.** 2001. SJL/J mice are highly susceptible to infection by mouse adenovirus type 1. J. Virol. **75:**12039–12046.
41. **Szomolanyi-Tsuda, E., J. D. Brien, J. E. Dorgan, R. L. Garcea, R. T. Woodland, and R. M. Welsh.** 2001. Antiviral T-cell-independent type 2 antibody responses induced *in vivo* in the absence of T and NK cells. Virology **280:**160–168.
42. **Szomolanyi-Tsuda, E., and R. M. Welsh.** 1996. T cell-independent antibody-mediated clearance of polyomavirus in T cell-deficient mice. J. Exp. Med. **183:**403–411.
43. **Walls, T., A. G. Shankar, and D. Shingadia.** 2003. Adenovirus: an increasingly important pathogen in paediatric bone marrow transplant patients. Lancet Infect. Dis. **3:**79–86.
44. **Wang, W. H., and H. L. Wang.** 2003. Fulminant adenovirus hepatitis following bone marrow transplantation. A case report and brief review of the literature. Arch. Pathol. Lab. Med. **127:**e246–248.
45. **Watson, V. E., L. L. Hill, L. B. Owen-Schaub, D. W. Davis, D. J. McConkey, C. Jagannath, R. L. J. Hunter, and J. K. Actor.** 2000. Apoptosis in mycobacterium tuberculosis infection in mice exhibiting varied immunopathology. J. Pathol. **190:**211–220.